Plant Molecular Biology (2006) 60:583–597
DOI 10.1007/s11103-005-5082-x

Expression analysis of the *AtMLO* gene family encoding plant-specific seven-transmembrane domain proteins

Zhongying Chen[1], H. Andreas Hartmann[2], Ming-Jing Wu[1], Erin J. Friedman[1], Jin-Gui Chen[1,4], Matthew Pulley[1], Paul Schulze-Lefert[2], Ralph Panstruga[2] and Alan M. Jones[1,3,*]

[1]*Department of Biology, The University of North Carolina at Chapel Hill, Chapel Hill, NC 27599, USA (*author for correspondence; e-mail alan_jones@unc.edu);* [2]*Department of Plant–Microbe Interactions, Max-Planck Institute for Plant Breeding Research, Carl-von-Linné-Weg 10, Cologne, D-50829, Germany;* [3]*Department of Pharmacology, The University of North Carolina at Chapel Hill, Chapel Hill, NC 27599, USA;* [4]*Department of Botany, University of British Columbia, 6270 University Boulevard, Vancouver, B.C. V6T 1Z4, Canada*

Received 28 June 2005; accepted in revised form 12 November 2005

Key words: *Arabidopsis thaliana*, GUS staining, heterotrimeric G-protein, microarray, MLO, RT-PCR

Abstract

The Arabidopsis (*Arabidopsis thaliana*) genome contains 15 genes encoding protein homologs of the barley mildew resistance locus o (MLO) protein biochemically shown to have a seven-transmembrane domain topology and localize to the plasma membrane. Towards elucidating the functions of MLOs, the largest family of seven-transmembrane domain proteins specific to plants, we comprehensively determined *AtMLO* gene expression patterns by a combination of experimental and *in silico* studies. Experimentation comprised analyses of transgenic Arabidopsis lines bearing promoter::β-glucuronidase (*GUS*) transcriptional fusions as well as semi-quantitative determination of transcripts by reverse transcription coupled to polymerase chain reaction (RT-PCR). These results were combined with information extracted from public gene profiling databases, and compared to the expression patterns of genes encoding the heterotrimeric G-protein subunits. We found that each *AtMLO* gene has a unique expression pattern and is regulated differently by a variety of biotic and/or abiotic stimuli, suggesting that AtMLO proteins function in diverse developmental and response processes. The expression of several phylogenetically closely-related *AtMLO* genes showed similar or overlapping tissue specificity and analogous responsiveness to external stimuli, suggesting functional redundancy, co-function, or antagonistic function(s).

Abbreviations: AGB1, the Arabidopsis Gβ subunit; AGG1, the Arabidopsis Gγ subunit1; AGG2, the Arabidopsis Gγ subunit2; FRET, Förster/Fluorescence Resonance Energy Transfer; GCR1, G-Coupled Receptor1; GPA1, the Arabidopsis Gα subunit; GPCRs, G-protein coupled receptors; GUS, β-glucuronidase; MLO, mildew resistance locus o; RGS1, Regulator of G-protein Signaling; 7TM, seven-transmembrane

Introduction

Multi-cellular organisms evolved mechanisms to sense both intra- and extra-cellular signals to achieve coordinated development and to respond properly to environmental cues. The seven-transmembrane (7TM) domain G-protein coupled receptors (GPCRs), which link diverse extracellular

stimuli to intracellular signaling networks via heterotrimetric G-proteins, represent the largest family dedicated to recognizing extracellular messengers (Bockaert and Pin, 1999). There are approximately 1000 members in vertebrates, and over 5% of the genome of *Caenorhabditis elegans* encodes GPCRs (Bockaert and Pin, 1999).

However, the genome of Arabidopsis (*Arabidopsis thaliana*) may encode far fewer presumptive 7TM domain proteins (Devoto *et al*., 1999). Among the predicted 7TM domain proteins, only two proteins, a putative plant GPCR protein, G-Coupled Receptor1 (GCR1), and an unusual Regulator of G-protein Signaling protein (AtRGS1), have been reported to be involved in G-protein signaling (Josefsson and Rask, 1997; Chen *et al*., 2003; Pandey and Assmann, 2004), yet their role as GPCR still awaits testing. Furthermore, the predicted heptahelical structure of GCR1 and AtRGS1 has not been confirmed experimentally.

The largest 7TM protein family in Arabidopsis is comprised of 15 members having significant sequence homology to a barley protein encoded by the mildew resistance locus o (*MLO*) gene. Accordingly, respective genes were designated *AtMLO*s (Devoto *et al*., 1999, 2003). Topology and subcellular localization studies showed barley MLO is plasma membrane delimited via its 7TM domains with the N-terminus positioned extracellularly and the C-terminus intracellularly like metazoan GPCRs (Devoto *et al*., 1999). Recent evidence obtained using FRET (Förster/Fluorescence Resonance Energy Transfer) analysis further revealed preliminary evidence for *in planta* MLO-dimerization/oligomerization (Elliott *et al*., 2005).

The biological functions of MLO proteins are largely unknown. MLO proteins are unique to plant taxa, dating back to early land-plant evolution (Devoto *et al*., 2003). In barley, plants carrying homozygous recessive *mlo* alleles are resistant to the biotrophic powdery mildew fungus, *Blumeria graminis* f. sp. *hordei*. This phenotype indicates a role of MLO in pathogen-related functions, possibly by modulating plant defense (Büschges *et al*., 1997). Consistent with an involvement in plant–microbe interactions, *MLO* expression is induced upon biotic and abiotic stress stimuli (Piffanelli *et al*., 2002). However, mediating disease susceptibility is unlikely the primary function of MLO. Rather, a yet unknown MLO-mediated host process may be usurped by the fungal pathogen for successful colonization. This is reminiscent of human diseases like AIDS, malaria and pneumonia (Panstruga and Schulze-Lefert, 2003), which are caused by pathogens requiring the presence of specific 7TM domain proteins in host cells for successful infections (Pease and Murphy, 1998). The function of barley MLO in mediating disease susceptibility appears to be independent of heterotrimeric G-proteins (Kim *et al*., 2002). However, a functional contribution of heterotrimeric G-proteins remains a possibility for unknown primary tasks of barley MLO and other MLO proteins (Panstruga and Schulze-Lefert, 2003).

Towards understanding the biological functions of AtMLO proteins, we determined expression patterns of *AtMLO* genes by performing promoter::*GUS* studies and reverse transcription coupled to polymerase chain reaction (RT-PCR) of the entire gene family. We also analyzed gene expression information from public gene profiling databases and examined 5′ upstream sequences of *AtMLO* genes for the presence of known regulatory elements. Our results indicate that each *AtMLO* gene has a unique expression pattern and is regulated differently by a variety of stimuli, suggesting that AtMLOs function in diverse developmental and response processes.

Materials and methods

*Generation of promoter::*GUS *constructs and transformation of* Arabidopsis

Based on the information provided by the TAIR web site (http://www.arabidopsis.org/, last modified on August 8th 2005), DNA fragments covering 5′ upstream (in the context of this study operationally defined as promoter) regions of *AtMLO*s and genes encoding G-protein subunits AGB1, AGG1 and AGG2 were each amplified from genomic DNA of wild type Arabidopsis (*Arabidopsis thaliana;* Col-0 ecotype) by using the primers listed in Table 1. Primers were generally designed to cover the 5′ upstream region of each gene starting immediately upstream of the start codon up to the end of the next gene located 5′ of the gene under consideration. The constructs were made in the following way: for *AtMLO2*,

Table 1. PCR primers used for amplifying regulatory regions of *AtMLO* genes, *AGB1, AGG1* and *AGG2.*

AGI	Gene	Primers[a]		Size (bp)[b]
		Forward	Reverse	
At4g02600	*AtMLO1*	5′-cacccaccCAAGTTTTGTTTTGATAA-3′	5′-ACCCATTTTACTTCTCACACCAGAGAG-3′	2299
At1g11310	*AtMLO2*	5′-AACACCGAAGCAATTGGGTCCATC-3′	5′-TGATCTGCCATggGAGCTTAATCCTAAG-3′	3404
At3g45290	*AtMLO3*	5′-ATCAATGACCGGCATATCTACAAG-3′	5′-ccatggCTTTATATTTTTCCCGGTGACTG-3′	4294
At1g11000	*AtMLO4*	5′-GAATTCATGACACACCAAATGTTC-3′	5′-ccatggCCGGCGAGGAACTTTTCTC-3′	2055
At2g33670	*AtMLO5*	5′-GCCTACTGATTCTCAACTGCACAG-3′	5′-TCCAGCCATggTTTCTTTAACGAAATTG-3′	2955
At1g61560	*AtMLO6*	5′-AAAATCATTAGAATTCCTATAATG-3′	5′-CCGCCATggGAACTCACAGAACAGTTCC-3′	1762
At2g17430	*AtMLO7*	5′-caccAGAAGCTGTAGGAGAAGGATCCAT-3′	5′-GAGTGAAGGAAATGAGAGGTGAGA-3′	1798
At2g17480	*AtMLO8*	5′-caccTTGTCTCCAACCAAATGG-3′	5′-AACTCCGCGTTATTTTAGTTTGGC-3′	2383
At1g42560	*AtMLO9*	5′-AAAACTAGGCATGACCATTGTTAC-3′	5′-ccatggCTTAAAACCGTGATGATTATC-3′	2076
At5g65970	*AtMLO10*	5′-TCCAACAACTCTAAGAAACCCATC-3′	5′-gatcgATGGTAGCCAAAAGAAGAAAATC-3′	2061
At5g53760	*AtMLO11*	5′-caccCTGTTTCACAAGAATTCACTATTC-3′	5′-TCCCATTTCTTTTAAAGTCTGATTCTTC-3′	2066
At2g39200	*AtMLO12*	5′-gagctcCTGAAGAAACACTCATTAGTAG-3′	5′-TTGCCATggATTTCACTGCTCAAAACTC-3′	3570
At4g24250	*AtMLO13*	5′-CTTTCTTAGCGGCACTATTCAGTG-3′	5′-ccatggCTGCACCTCCAAGATGGAGAC-3′	947
At1g16700	*AtMLO14*	5′-caccGGTGGAAGCTTTGAAG-3′	5′-TTTCTTCAACCGAATTCTTTATGAACA-3′	2618
At2g44110	*AtMLO15*	5′-caccTGAAAGCTTCCTTCTTTATCTT-3′	5′-TTTTTTGCTCCGGTGATTCGT-3′	910
At4g34460	*AGB1*	5′-caccGCCCATGAATCAAAAACCTAA-3′	5′-TCCGGGATCAGACTTAGGCTT-3′	755
At3g63420	*AGG1*	5′-caccGCCGAGGAATCGATCTGGCAT-3′	5′-TTGCAGAAAAATGCCAAAACGCCCAA-3′	351
At3g22942	*AGG2*	5′-caccCTTGGCTCGTACTTCGAT-3′	5′-CAAAATTTCTCGAATTCAACCCTCA-3′	1757

[a] Lower case letters are sequences do not match with genomic DNA; Underlined are restriction sites.
[b] Size of amplified regulatory regions.

AtMLO3, *AtMLO4*, *AtMLO5*, *AtMLO6*, *AtMLO9*, *AtMLO10* and *AtMLO13*, PCR products (using *pfu* or *pwo* polymerase) were cloned into the *Sma*I site of pBluescript. Subsequently, they were excised as *Eco*RI/*Nco*I (for *AtMLO2*, *AtMLO3*, *AtMLO4*, *AtMLO5*, *AtMLO6*, *AtMLO9* and *AtMLO13*), *Eco*RI/*Cla*I (for *AtMLO10*), or *Sac*I/*Nco*I (for *AtMLO12*) fragments and co-ligated with either a *Nco*I/*Hin*dIII *GUS* fragment (excised from pSLJ4D4 (Jones *et al*., 1992); for *AtMLO2*, *AtMLO3*, *AtMLO4*, *AtMLO5*, *AtMLO6*, *AtMLO9*, *AtMLO12* and *AtMLO13*) or a *Cla*I/*Hin*dIII *GUS* fragment (excised from pSLJ4K1 (Jones *et al*., 1992); for *AtMLO10*), into the binary vector pPZP211 (GenBank accession number U10490). For *AtMLO1*, *AtMLO7*, *AtMLO8*, *AtMLO11*, *AtMLO14* and *AtMLO15*, PCR products (Phusion, Finnzymes, Espoo, Finland) were cloned into the pENTR/D-TOPO vector (Invitrogen, Carlsbad, CA), then moved into the Gateway destination binary vector, pGWB3 (Research Institute of Molecular Genetics, Matsue, Japan) by an LR recombination reaction. All these constructs were transformed into wild type Arabidopsis plants of Col-0 ecotype via floral dip as described by Clough and Bent (1998). The transgenic plants were selected for kanamycin-resistance, and the presence of the corresponding promoter::*GUS* gene was confirmed by PCR. For *AGB1*, *AGG1* and *AGG2*, PCR products were cloned into the pENTR/D-TOPO vector (Invitrogen, Carlsbad, CA), then moved into the Gateway destination binary vector pBGWFS7 (Karimi *et al*., 2002). The constructs were transformed into *A. thaliana* (Col-0 ecotype) by *Agrobacterium*-mediated transformation (Bechtold and Pelletier, 1998).

Plant materials

Seeds of *AtMLO* promoter::*GUS* lines were sterilized in ethanol as described by Turk *et al*. (2003), plated on ½ MS media supplemented with 1% sucrose, and stratified at 4 °C for 2 days. The seedlings were then grown at 24 °C either in dark for 3 days, or under constant light for 10 days before subjected to GUS staining. Seeds were also planted on soil, stratified at 4 °C for 2 days, and grown under 24 °C 8/16 h light/dark cycles for 15 days. Some of the 15-day-old plants were gently removed from soil, rinsed in water, and subjected to GUS staining. Fifteen-day-old plants were then moved to a green house with 16/8 h light/dark cycles. Upon request, all novel materials described in this publication will be made available in a timely manner for non-commercial research purposes, subject to the requisite permission from any third-party owners of all or parts of the material. Obtaining any permission will be the responsibility of the requestor.

GUS staining assays

GUS histochemical staining of transgenic Arabidopsis plants containing *AtMLO* promoter::*GUS* fusion constructs was performed as described by Malamy and Benfey (1997). Briefly, seedlings or excised tissues were vacuum infiltrated for 30 s with freshly-prepared staining solution [100 mM Tris–HCl (pH7.5), 50 mM NaCl, 2 mM potassium ferricyanide, 20%(v/v) methanol, 0.001%(v/v) Triton X-100 and 1 mM 5-bromo-4-chloro-3-indolyl β-D-glucuronide (X-Gluc; Rose Scientific Ltd., Edmonton, Alberta, Canada)]. After incubation at 37 °C in dark overnight, seedlings or tissues were cleared in 70% ethanol, examined with a dissecting or compound microscope, and photographed with a digital camera. Images shown represent the typical results of at least three independent lines for each construct.

Phylogenetic analysis of AtMLO proteins

The Phylip 3.63 software package (http://evolution.gs.washington.edu/phylip.html) was used for phylogenetic analysis. AtMLO protein sequences were downloaded from http://www.ncbi.nlm.nih.gov/. The highly polymorphic N- and C-termini of AtMLO protein sequences aligned by CLUSTALW were removed before calculating phylogenetic relationships. Thereafter, the Seqboot, Protdist, Neighbor and Consense algorithms were sequentially applied to establish the phylogenetic consensus tree, using 100 replicates each for bootstrap support. This majority rule consensus tree based on neighbor-joining was fed as a user tree in ProtML (maximum likelihood inference of protein phylogeny) to re-estimate branch lengths. The final tree was visualized using TreeView 1.6.6.

RT-PCR

RNA was isolated using the TRIzol Reagent (Invitrogen, Carlsbad, CA) from tissues of wild

type Col-0 Arabidopsis plants, including stems, leaves and inflorescence of mature plants, as well as roots and shoots of 10-day-old seedlings grown on ½ MS media supplemented with 1% sucrose under constant light. Reverse transcription reaction was carried out by using the ThermoScript™ RT-PCR System (Invitrogen, Carlsbad, CA). Complementary DNA derived from about 2 μg of total RNA was used for PCR reactions. *AtMLO* cDNAs were amplified for 40 cycles, and *AtACT2* cDNA were amplified for 30 cycles. Primers used are listed in Supplemental Table 1.

Analysis of regulated gene expression using public gene profiling data

Gene expression data were downloaded as an Excel file from Genevestigator (version September 2005) using the Digital Northern server. Selected profiles with replications were used such that the average of expression levels was used for comparison. As recommended by the server, expression data with a *P*-value >0.06 were marked as absent (signals not significantly higher than background), and were not used to compare with other absent data. Only responses with expression levels altered by more than two-fold are shown in Table 3.

Web-based tool for Arabidopsis *MLOs and G-proteins*

An online gene expression database search tool was created as a Microsoft Access database-driven web utility based on ASP.NET and written in VB.NET and HTML. The tool was designed to allow researchers to collect data in a centrally-stored database while providing searchable data in a manner customized by the user. The user may search the database by gene or by tissue of interest. The page then requests relevant data from the database and displays it accordingly. This database will be updated to reflect any gene investigated by the community. The tissue search begins with a dynamic Macromedia Flash movie of Arabidopsis plants at several different developmental stages. Once a tissue has been selected, the link passes a specific value to an overall results page, which subsequently displays any relevant genes expressed in the tissue of interest. For each gene, expression images and text detailing specific locations within each tissue are displayed. To initiate a search by gene, the user selects a gene from a drop-down list populated from the database. The resulting page displays results profiling that gene. Finally, both the tissue and gene results pages are cross-referenced. This utility is available at http://www.bio.unc.edu/faculty/jones/lab/MLO/search.aspx.

Results

Tissue-specific expression of AtMLO *genes*

To determine the expression patterns of *AtMLO* genes, we isolated respective regulatory regions of *AtMLO* genes upstream to the predicted start codon, transcriptionally fused these promoters to the reporter gene β-glucuronidase (*GUS*), and transformed these chimeric genes into Arabidopsis. At least three independent promoter::*GUS* lines were characterized for each construct. Tissue-specific *AtMLO* expression at different developmental stages was assessed from 3-day-old etiolated seedlings (grown on ½ MS 1% sucrose plates), 10-day-old light-grown seedlings (grown on ½ MS 1% sucrose plates), 15-day-old plant (grown in soil), and leaves and inflorescence from soil grown mature plants. Staining patterns of *AtMLO* promoter::*GUS* lines in selected organs are shown in Figure 1. Detailed staining patterns of promoter::*GUS* lines are shown in Supplemental Figures 1–15 and summarized in Table 2. The data are also provided in a user-interactive database (http://www.bio.unc.edu/faculty/jones/lab/MLO/search.aspx).

No two *AtMLO* genes had identical expression profiles, suggesting distinct functions of AtMLO proteins. On the other hand, many *AtMLO* genes have overlapping expression patterns. Specifically, *AtMLO1*, *AtMLO2*, *AtMLO3*, *AtMLO4*, *AtMLO6*, *AtMLO9*, *AtMLO10*, *AtMLO11*, *AtMLO12* and *AtMLO13* genes showed expression in vascular tissues of leaf and/or cotyledon. *AtMLO1*, *AtMLO2*, *AtMLO3*, *AtMLO4*, *AtMLO9*, *AtMLO10*, *AtMLO11*, *AtMLO12* and *AtMLO13* genes also exhibited expression in root vascular tissues. Promoter::*GUS* lines of *AtMLO1*, *AtMLO3*, *AtMLO5*, *AtMLO7*, *AtMLO9* and *AtMLO15* showed positive GUS staining in pollen grains. Additionally, many *AtMLO* genes, including *AtMLO2*, *AtMLO3*, *AtMLO4*, *AtMLO6*,

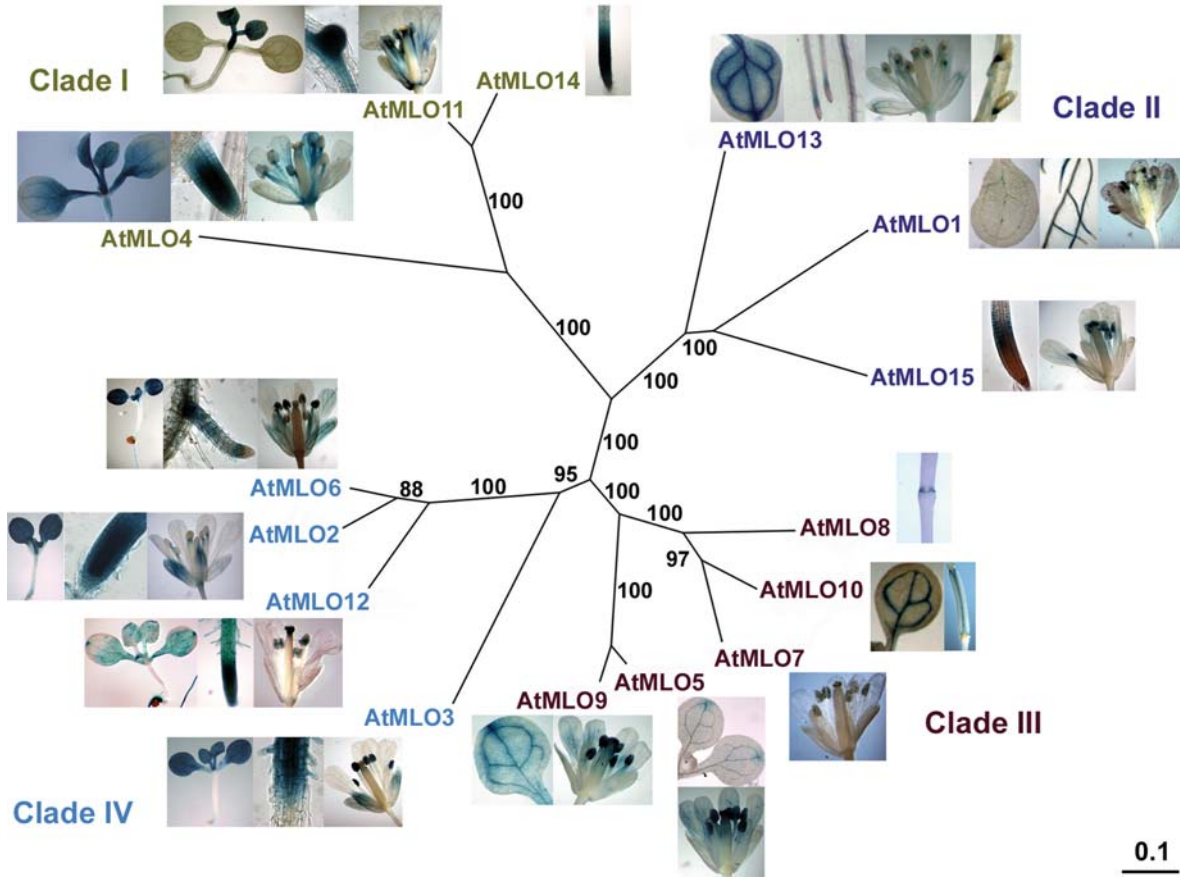

Figure 1. Phylogenetic analysis of Arabidopsis MLO protein family members and tissue-specific expression of *AtMLO* genes. The unrooted phylogenetic tree represents a consensus tree with bootstrap values above branches indicating the number of replicates (out of 100) that support the respective branch. The scale bar (right bottom corner) indicates the number of amino acid substitutions per site. GUS staining pattern of *AtMLO* promoter::*GUS* lines in selected tissues are shown adjacent to the corresponding AtMLO proteins to highlight similar and distinct expression of *AtMLO* genes in clades. Comprehensive GUS staining patterns for *AtMLO* promoter::*GUS* lines are provided in Supplemental Figures 1–15.

AtMLO8, *AtMLO9*, *AtMLO11*, *AtMLO12* and *AtMLO13*, exhibited varying degrees of expression at the abscission zone of the floral organs (Table 2, Supplemental Figures 1–15). Overlapping expression of *AtMLO* genes suggests potential functional redundancy among the AtMLO proteins, putative co-function or antagonistic function of AtMLOs, e.g. by forming heterodimers or oligomers. The unique expression of *AtMLO10* in valve margins of elongating siliques and *AtMLO13* in funuculus suggest a possible involvement of AtMLO10 and AtMLO13 in the processes of dehiscence and seed detachment, respectively (Figure 1, Supplemental Figures 10M and 13M).

The expression of many *AtMLO* genes displayed developmental regulation. *AtMLO3* expressed in trichomes of young leaves but exhibited preferential expression in vascular tissues of older leaves. *AtMLO10* expression in inflorescence was limited to valve margins of elongating siliques but not in young carpels or in mature siliques. The expression patterns of *AtMLO2*, *AtMLO3*, *AtMLO4*, *AtMLO6*, *AtMLO8*, *AtMLO9*, *AtMLO11*, *AtMLO12* and *AtMLO13* at the abscission zone of the floral organs were observed only in flowers during or after the shedding process, but not in flowers of early stages (Supplemental Figures 2–4, 6, 8, 9, 11–13).

We also followed *AtMLO* gene expression in several organs by performing semi-quantitative RT-PCR using primer pairs specific for each *AtMLO* gene (Supplemental Table 1, Figure 2)

Table 2. Staining profile of *AtMLO* promoter::*GUS* transgenic plants.

Organs and tissues	*AtMLO* promoter														
	1	*2*	*3*	*4*	*5*	*6*	*7*	*8*	*9*	*10*	*11*	*12*	*13*	*14*	*15*
Root	√	√	√	√		√			√	√	√	√	√	√	√
Tip		+		+							+	+		+	
Vascular	+	+	+	+					+	+	+	+	+		
Epidermis		+	+			+						+		+	+
Leaf and cotyledon	√	√	√	√	√	√			√	√	√	√	√		
Veins	+	+	+	+		+			+	+	+	+	+		
Hydathode		+			+	+			+			+			
Trichome		+	+			+					+	+			
Petiole	+	+	+	+		+			+	+	+	+	+		
Stem	√	√	√	√				√	√	√			√		
Vascular	+	+								+			+		
Inflorescence	√	√	√	√	√	√	√	√	√	√	√	√	√		√
Sepal		+	+	+		+						+	+		
Petal						+			+				+		
Filament		+	+	+		+			+		+		+		
Anther			+		+	+			+			+			+
Pollen	+		+		+		+		+						+
Carpel	+	+	+	+	+	+			+		+	+	+		+
The abscission zone		+	+	+		+		+	+		+	+	+		
Silique valve margin										+					
Funiculus													+		

The presence of GUS staining in root, leaf and stem tissues of 10-day-old seedlings, and in inflorescence tissues of mature plants was summarized in this table using √ indicating a positive staining in organs and using + indicating a positive staining in tissues.

and extracted replicated data from public databases (https://www.genevestigator.ethz.ch, Supplemental Table 2 and Figure 3). In many cases, organ- or tissue-specific expression of *AtMLO* genes obtained from RT-PCR and microarray experiments was consistent with patterns observed from the promoter::*GUS* lines. For instance, strong expression of *AtMLO5* and *AtMLO9* in inflorescence was found by all three approaches. However, discrepancies among results obtained using different approaches were also found. For example, microarray analysis suggested high level of *AtMLO14* expression in pollen, however, both GUS staining and RT-PCR suggested highest *AtMLO14* expression in roots, but no expression in inflorescence tissues. *AtMLO15* promoter::*GUS* lines showed staining in root and inflorescence tissues (Figure 1, Supplemental Figure 15), however, RT-PCR and microarray experiments only detected *AtMLO15* expression in roots (Figures 2 and 3). Additionally, RT-PCR and microarray experiments suggested that *AtMLO7* and *AtMLO8* are expressed in a broader range of tissues than suggested by GUS staining experiments. In the case of *AtMLO8*, since microarray experiments suggest that it is induced by wounding (described later), the ubiquitous *AtMLO8* expression detected in RT-PCR and microarray experiments may be due to induction during tissue collection. In fact, we occasionally observed asymmetric staining in tissues of *AtMLO8*::*GUS* lines (Supplemental Figure 8A–D), suggesting wound-induced expression. These discrepancies highlight the need for multiple approaches when assessing gene expression patterns.

Overlapping tissue-specific expression of closely related AtMLO *genes*

To establish the relationship of AtMLOs, protein sequences lacking the hypervariable amino and carboxy terminal domains were subjected to phylogenetic analysis resulting in an unrooted phylogenetic tree (Figure 1 and Devoto *et al.*, 2003). Adopting the nomenclature put forward by Devoto *et al.* (2003), the 15 AtMLO proteins fall into putative clades I through IV. Note that in an unrooted tree the possibility that the root position is within an apparent clade cannot be excluded.

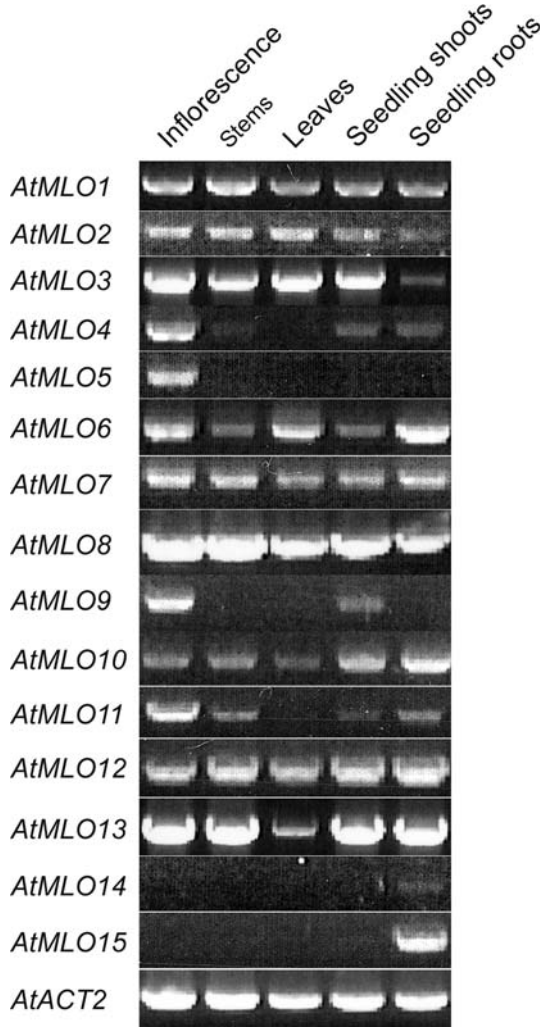

Figure 2. RT-PCR analysis of the expression of *AtMLO* genes in different tissues. RNA was isolated from stems, leaves and inflorescence of mature plants, and from roots and shoots of 10-day-old seedlings grown on ½ MS media supplemented with 1% sucrose under constant light. After the reverse transcription reaction, *AtMLO* cDNAs were amplified for 40 cycles, and *AtACT2* cDNA (encoding Actin2 protein, serving as a control for ubiquitous constitutive expression) were amplified for 30 cycles. Similar results were obtained in two other independent experiments.

All genes in clade I expressed in roots, preferentially in root tips. *AtMLO4* and *AtMLO11* exhibited similar expression in leaf and inflorescence tissues, although *AtMLO4* was distinguished from *AtMLO11* by expression in cotyledons (Figure 1, Supplemental Figures 4, 11, and 14). Taken together, genes in this clade have overlapping tissue-specific expression, and the overlap between expression patterns of *AtMLO4* and *AtMLO11* is the most extensive.

Genes in clade II exhibited expression in both vegetative and floral organs (Figure 1, Supplemental Figures 1, 13, and 15). However, *AtMLO13* and *AtMLO15* showed distinct tissue-specificity. In roots, *AtMLO13* expressed in vascular tissues, whereas *AtMLO15* expressed in root tips at the early elongation zone. In flowers, *AtMLO13* expressed in the vasculature of floral organs, whereas *AtMLO15* preferentially expressed in pollen grains and papilla cells (Figure 1, Supplemental Figures 13 and 15). Interestingly, tissue-specificity of *AtMLO1* was similar to *AtMLO13* in vegetative organs, but similar to *AtMLO15* in floral organs (Supplemental Figures 1, 13, and 15), marking overlapped expression between *AtMLO1* and *AtMLO13*, and between *AtMLO1* and *AtMLO15*.

In clade III, AtMLO5 and AtMLO9 proteins are the most closely related, and we found that the corresponding genes also shared the most similar expression patterns suggesting a recent gene duplication event. Both genes expressed in leaf hydathodes and had strong expression in anthers, pollen grains, and styles (Supplemental Figures 5 and 9). In contrast, other genes in clade III exhibited very diverse expression patterns. *AtMLO7* expressed in pollen grains, *AtMLO8* expressed in pedicle–stem junction sites and the abscission zones of the floral organs, whereas *AtMLO10* expressed in vascular tissues of vegetative organs and in the valve margins of elongating fruits (Supplemental Figures 7, 8, and 10).

Clade IV was distinct from the other three clades in that all members exhibited relatively strong expression in cotyledons and leaves, in addition to expression in root and floral organs (Figure 1, Supplemental Figures 2, 3, 6 and 12, Supplemental Table 2). Meanwhile, each member had unique features in their tissue-specificity. For example, unlike other members, *AtMLO2* was not expressed in anthers or pollen grains, whereas *AtMLO3* can be distinguished from others in that its root expression starts from the differentiation zone (Supplemental Figures 2 and 3).

Similarity in expression patterns of *AtMlo5* and *AtMlo9*, and of *AtMlo2* and *AtMlo3* were confirmed by analyzing replicated microarray data (Figure 3, Zimmermann *et al*., 2004). The observation that these closely-related *AtMLO*

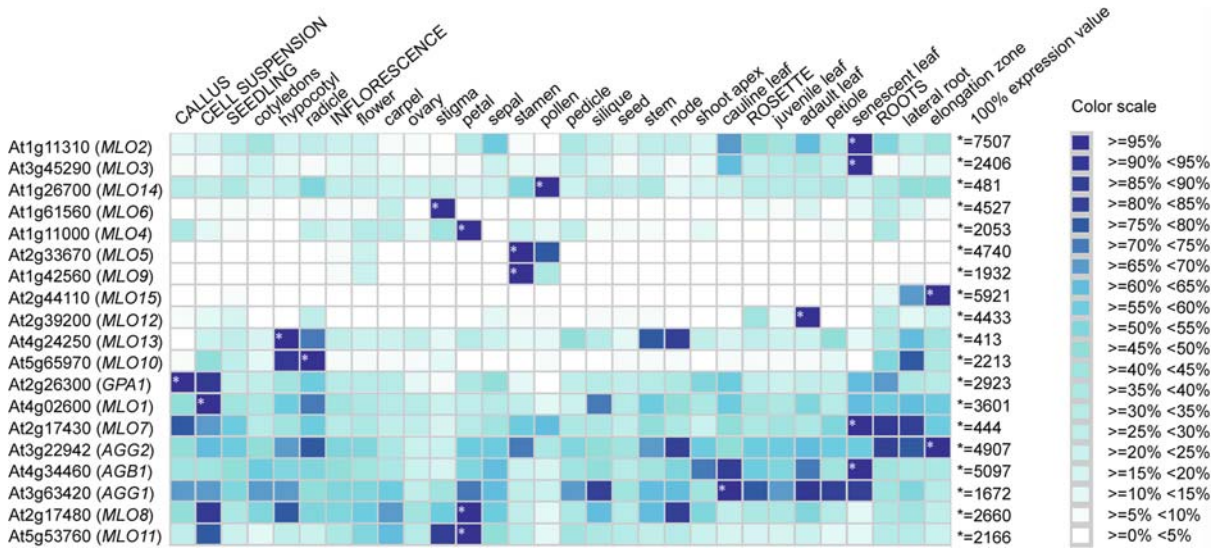

Figure 3. Expression of *AtMLOs* and genes encoding G-protein subunits in plant organs. Gene expression profiles based on microarray data were clustered according to similarity in expression patterns (Zimmermann *et al*., 2004). The figure was modified from an output result of Meta-Analyzer of Genevestigator (last modified in September 2005), which illustrates different expression levels of each gene in different organs, and groups of genes with similar expression patterns by Hierarchical Clustering. Hierarchical Clustering results were generated by default settings that calculate Pairwise Euclidean distances and uses the Average Linkage method. Results are given as heat maps in blue/white coding that reflects absolute signal values, where darker represent stronger expression. For the blue–white scale, all gene-level profiles were normalized for coloring such that for each gene the highest signal intensity obtains value 100% (dark blue, marked with *, for which the actual expression value was given in the figure) and absence of signal obtains value 0% (white).

genes have similar or overlapping expression patterns thus provides further evidence suggesting functional relatedness of respective AtMLO proteins.

Regulated expression of AtMLO *genes*

As summarized in Table 3, *AtMLO* gene expression data in response to various cues was extracted from public databases (Supplemental Table 2) and the average of expression levels of replicated microarray data was used for comparison.

The steady-state level of *AtMLO1*, *AtMLO2*, *AtMLO4*, *AtMLO6*, *AtMLO7*, *AtMLO8* and *AtMLO12* transcripts increased in 7-day-old seedlings treated with cycloheximide, suggesting that the transcription of these genes is controlled by short-lived negative regulators. Additionally, treatment of 7-day-old seedlings with the ethylene perception inhibitor $AgNO_3$ dramatically induced the expression of *AtMLO2*, *AtMLO3*, *AtMLO6* and *AtMLO12*, but suppressed the expression of *AtMLO15*. Since none of the above mentioned *AtMLO* genes exhibited altered expression in the presence of the ethylene precursor ACC (Supplemental Table 2), the altered expression of these *AtMLO* genes by $AgNO_3$ is likely due to heavy metal toxicity.

As previously shown for barley *MLO* (Piffanelli *et al*., 2002), the expression of many *AtMLO* genes was affected by biotic and/or abiotic stresses. *AtMLO2*, *AtMLO3*, *AtMLO6* and *AtMLO12*, which comprise clade IV and have abundant expression in leaf tissues, appear to be the most responsive *AtMLO* genes under biotic stresses. All four *AtMLOs* were induced by the biotrophic fungal pathogen *Erysiphe cichoracearum*. *AtMLO3* and *AtMLO12* were induced by the related fungal pathogen *Golovinomyces* (formerly designated as *Erysiphe orontii*). *AtMLO6* and *AtMLO12* were induced by the hemibiotrophic oomycete pathogen *Phytophtora infestans* and the necrotrophic fungal pathogen *Botrytis cinerea*. Additionally, the expression of *AtMLO2*, *AtMLO3*, *AtMLO6* and *AtMLO12* genes was altered by the bacterial pathogen *Pseudomonas syringae* depending on the specific strain used. These findings suggest that

Table 3. Altered expression of *AtMLO* genes and genes encoding G-protein subunits in response to stimuli.

Treatments	*AtMLO* genes												*GPA1*	*AGB1*	*AGG1*
	1	*2*	*3*	*4*	*6*	*7*	*8*	*10*	*11*	*12*	*13*	*15*			
Chemicals															
[113][a] Cycloheximide (3h)[b]	**2.6**[c]	**5.0**		**6.4**	**11.1**	**2.0**	**5.8**			**25.5**		−2.1	**5.2**	**2.8**	**2.2**
[113] $AgNO_3$ (3h)		**2.0**	**3.1**		**3.8**					**2.1**		−11.0			
Biotic stresses															
Fungal pathogens															
[86] *Erysiphe cichoracearum* (8–12h)		**2.6**	**6.1**		**4.5**					**2.4**					**2.1**
[146] *Erysiphe orontii* (120h)			**2.5**							**8.5**					
[108] *Phytophtora infestans* (6h)					**4.3**					**2.2**					**2.3**
[147] *Botrytis cinerea* (48h)					**4.1**					**2.5**					
The bacterial pathogen *Pseudomonas syringae*															
[106] Vir (24h)			−2.1		**2.8**					**3.8**			**4.9**		
[106] Avr (24h)		**2.0**	−2.2		**4.4**					**4.0**			**2.7**		
[106] HrcC (24h)		**2.2**	**2.5**		**3.1**					**13.1**					
[106] Non-host (24h)		**2.6**			**3.9**					**10.8**					
Abiotic stresses															
In leaves															
[121] Cold (12h)		−2.9					**2.2**			**2.9**			−2.8		
[122] Osmotic stress (24h)			**3.2**		**2.2**				−2.1	**2.3**				**2.4**	
[123] Salt (6h)									**2.0**						
[127] Wound (1h)					**2.5**		**2.5**[d]		**3.1**	**5.1**					
In roots															
[121] Cold (12h)						−2.5[e]	**2.3**			**2.0**					
[122] Osmotic stress (12h)				−2.5				−2.5		−2.1		−3.7			
[123] Salt (6h)				**2.8**	**3.9**		**2.9**	-8.4	**2.3**	**16.8**	**2.1**	-4.2	**2.1**		

This table is generated based on information extracted from public gene profiling databases obtained from the GENEVESTIGATOR web site. Only profiles with replications are analyzed and only significant responses with expression levels altered by more than two-fold are shown. All data were generated using the 22K Affymetrix ATH1 Arabidopsis Genome array. The expression of *AtMLO5, AtMLO9, AtMLO14* and *AGG2* was not altered for more than two-fold in any of these experiments, and therefore is not shown in this table.

[a] Experiment ID, detailed information about treatment in each experiment can be obtained from the GENEVESTIGATOR web site.
[b] Sampling hours after treatment.
[c] Positive numbers in bold show fold of increase in expression levels, negative numbers show fold of decrease in expression levels.
[d] Sampled at 30 min after treatment.
[e] Sampled at 24 h after treatment.

these genes are actively and precisely regulated during infections, indicating that they likely play important roles for disease/resistance.

Expression of *AtMLO* genes from multiple clades was affected by abiotic stresses. In leaves, the level of *AtMLO2* transcripts decreased, whereas those of *AtMLO8* and *AtMLO12* transcripts increased after cold treatment. *AtMLO3*, *AtMLO6* and *AtMLO12* transcript levels increased, whereas that of *AtMLO11* decreased after osmotic stress. Salt stress induces *AtMLO11*, and wounding induces *AtMLO6*, *AtMLO8*, *AtMLO11* and *AtMLO12*. In roots, cold stress induced *AtMLO8* and *AtMLO12* expression at 12 h, but suppressed *AtMLO7* expression at 24 h after treatment. Osmotic stress suppressed *AtMLO4*, *AtMLO10*, *AtMLO12* and *AtMLO15* transcripts. Salt stress induced *AtMLO4*, *AtMLO6*, *AtMLO8*, *AtMLO11*, *AtMLO12* and *AtMLO13*, but suppressed *AtMLO10* and *AtMLO15*.

Additionally, the expression of *AtMLO2* appears to be diurnally regulated (Supplemental Figure 16), whereas that of *AtMLO4* is repressed by light treatments (Supplemental Figure 17). Taken together, the expression of many *AtMLO* genes is regulated differently by a variety of biotic and abiotic stimuli, suggesting that AtMLO proteins function in diverse response processes. Additionally, clade IV genes exhibited analogous responsiveness to biotic and/or abiotic stimuli, providing further evidence for functional relatedness.

To gain insight on the molecular basis of regulated *AtMLO* gene expression, we performed searches for *cis*-elements in predicted or curated *AtMLO* promoter regions, using the Arabidopsis Gene Regulatory Information Server (AGRIS: http://arabidopsis.med.ohio-state.edu, version 4, Table 4), which contains *cis*-elements characterized from Arabidopsis (Davuluri *et al*., 2003), and using the Database of Plant *Cis*-acting Regulatory DNA Elements (PLACE, http://www.dna. affrc.go.jp/ PLACE, version 20.0, Supplemental Table 3), which contains *cis*-elements characterized from a variety of different plant species (Higo *et al*., 1999). Binding sites of bZIP, MYB and MYC transcription factors were found among promoter regions of *AtMLO* genes, in agreement with the microarray results indicating that the expression of many *AtMLO* genes was regulated by biotic and/or abiotic stresses. Additionally, microarray data indicated that the expression of *AtMLO4* was significantly repressed by light (Table 3), consistent with the presence of a G-Box (known to be over-represented in light-regulated genes; Hudson and Quail, 2003), and a SORLREP4 (Sequences Over-Represented in Light-REpressed Promoters; Hudson and Quail, 2003) *cis*-element in the curated *AtMLO4* promoter region (Table 4). However, inconsistencies between identified *cis*-elements and the microarray data were also found. For example, promoter regions of many *AtMLO* genes had binding site(s) of auxin response factors, but neither microarray or RT-PCR data displayed significant and reproducible auxin regulation on *AtMLO* expression (Supplemental Table 2 and data not shown). Additionally, promoter regions of *AtMLO1*, *AtMLO10* and *AtMLO15* have W-box motif at higher frequencies than expected, but none of these genes exhibited altered expression during pathogen infections (Tables 3 and 4). Apparently, although this promoter analysis may be helpful in identifying type of transcription factors involved in regulation, it is not reliable for predicting mode of regulation.

Expression of genes encoding subunits of heterotrimeric G-proteins

The 7TM domain topology and plasma membrane localization of MLO proteins make them candidate plant GPCRs. Spatiotemporal overlap in expression between genes encoding MLO proteins and G-protein subunits would be a prerequisite for a potential function of MLOs as GPCRs. The low complexity of the G-protein subunit family encoded by the Arabidopsis genome (comprising a single canonical Gα (GPA1) and Gβ (AGB1) subunits and only two Gγ (AGG1 and AGG2) subunits), renders spatially and temporally highly resolved comparisons with *AtMLO* expression patterns feasible. Immunolocalization of GPA1 was found in meristems, vascular tissues of leaves and roots, as well as inflorescence tissues (Weiss *et al*., 1993; Ma, 1994), whereas northern blot analyses of *AGB1, AGG1* and *AGG2* transcripts in organs suggested that these genes and *GPA1* have similar or overlapping expression patterns (Mason and Botella, 2000, 2001).

We determined *AGB1*, *AGG1* and *AGG2* expression by performing promoter::*GUS* analysis. *AGB1* exhibited ubiquitous expression in vegetative organs, and expression in stamens, stigma and the abscission zone of the floral organs (Supplemental Figure 18). *AGG1* is expressed in apical meristem, leaves, mature roots, the abscission zone of the floral organs and stamens (Supplemental Figure 19). GUS activity was detected in vegetative organs of *AGG2* promoter::*GUS* lines, including meristemeric tissues, leaves (preferentially in hydathods and vascular tissues) and the root stele (Supplemental Figure 20).

Similar ubiquitous expression of genes encoding G-protein subunits was also confirmed by analyzing public gene profiling databases (Figure 3). The extensive overlap among expression patterns of these G-protein subunits is consistent with the hypothesis that these proteins form heterotrimers for intracellular signaling.

The expression of genes encoding G-protein subunits is relatively stable under external changes, compared with *AtMLO* genes in clade IV (Table 3). The relative ubiquitous expression pattern of these subunits allows overlap with multiple *AtMLO*s, and makes co-functioning of G-proteins with AtMLOs spatially and temporally possible. However, whether MLO proteins function as GPCRs requires extensive testing.

Discussion

About 30% of Arabidopsis genes encode plant-specific proteins and proteins with unknown func-

Table 4. *Cis*-elements in *AtMLO* regulatory regions found by using the AGRIS server[a].

Name	*AtMLO* regulatory regions[b]															Consensus sequence	Expected frequency[c]
	1	*2*	*3*	*4*	*5*	*6*	*7*	*8*	*9*	*10*	*11*	*12*	*13*	*14*	*15*		
ABRE-like binding site motif				1												(C/G/T)ACGTG(G/T)(A/C)	0.2607[e]
AG BS in AP3			1													CCATTTTTAGT	0.0005
ARF binding site motif	2	1			1	1	1		2	3		1	1			TGTCTC	0.5371
ATB2/AtbZIP53/AtbZIP44/GBF5 BS in ProDH	2						1		1		1	1	1		1	ACTCAT	0.5371
ATHB2 binding site motif			1													CAAT(C/G)ATTG	0.0084
AtMYB2 BS in RD22												1				CTAACCA	0.1343
AtMYC2 BS in RD22	2	1	1	2			1		1		2	1		2		CACATG	0.5371
Bellringer/replumless/pennywise BS1 IN AG	1	1	2	1	1		5		2	1						AAATTAAA	0.0336
BoxII promoter motif				1		1								1	2	GGTTAA	0.5371
CBF1 BS in cor15a											1					TGGCCGAC	0.0336
CCA1 binding site motif	1					1		1	1						1	AA(A/C)AATCT	0.0671
CCA1 motif1 BS in CAB1								1								AAACAATCTA	0.0021
DPBF1&2 binding site motif	3	1	1	2			2		1	3	1	1		1		ACACNNG[d]	2.1484
E2F binding site motif													1			TTTCCCGC	0.0336
GATA promoter motif [LRE]	6	3	4	1	1	2	3	3	5	7		3	5	5	5	(A/T)GATA(G/A)	2.1484
G-box promoter motif [LRE]				1												CACGTG	0.1738[e]
GCC-box promoter motif													1			GCCGCC	0.5371
Hexamer promoter motif					1					1						CCGTCG	0.5371
Ibox promoter motif		2	1						1			1	1			GATAAG	0.5371
L1-box promoter motif										2	2	1		1		TAAATG(C/T)A	0.0671
LFY consensus BS motif	2	1		2	1		4		1	1	1		5		2	CCANTG	2.1484
LTRE promoter motif			1													ACCGACA	0.1343
MYB binding site promoter	2										1	1	2	1	1	(A/C)ACC(A/T)A(A/C)C	0.2686
MYB1 binding site motif														1		(A/C)TCC(A/T)ACC	0.1343
MYB4 binding site motif	1	1	2		1		1		1	2	4	1	3	1	1	A(A/C)C(A/T)A(A/C)C	1.0742
RAV1-A binding site motif	4	2	5	2	3		3	2	3	6	3	4	3			CAACA	2.1484
SORLREP1			1													TT(A/T)TACTAGT	0.0042

SORLREP2						1						1		1	ATAAAACGT	0.0084
SORLREP3							1				1				TGTATATAT	0.0084
SORLREP4			1												CTCCTAATT	0.0054[e]
SORLIP1	1					1		1				1		1	AGCCAC	0.5371
SORLIP2							1								GGGCC	2.1484
SORLIP5											1				GAGTGAG	0.1343
T-box promoter motif	1	1		2	3	1	2			4	4	1			ACTTTG	0.5371
TELO-box promoter motif				1							1				AAACCCTAA	0.0084
W-box promoter motif	4	3	2	2		5	4	3	2	7	1	2	1	1	5	TTGAC	2.1484
Z-box promoter motif											1					ATACGTGT	0.0336

[a] Last modified on May 9th, 2005.
[b] Regulatory regions cover a 712 bp, a 548 bp and a 910 bp fragments for *AtMLO4*, *AtMLO5* and *AtMLO15* respectively, and cover 1100 bp fragments for the rest *AtMLOs* 5′ to the translation start codon and the cureted or predicted 5′-untranslated regions of each gene.
[c] Expected number of random occurrence for a 1100 bp fragment if not specified.
[d] N = A/T/C/G.
[e] Expected number of random occurrence for a 712 bp fragment.

tions (The Arabidopsis Genome Initiative, 2000). Since function for these protein families cannot be gleaned from the studies of non-plant orthologs, in-depth functional analyses of these proteins presents a challenge requiring multiple experimental approaches. Although convergent evolution might have resulted in gene families encoding distinct proteins but fulfilling similar tasks in diverse kingdoms, plant-specific protein families can be assumed to function in many cases in developmental or adaptation processes that are specific to plant species. The systems biology approach requires determination of tissue-specificity and stimulus-dependent regulation of these genes which consequently drive the design of experiments to ultimately interpret the function of the encoded proteins.

We used the methods of promoter::*GUS* analysis, RT-PCR and *in silico* gene profiling to determine *AtMLO* expression. In general, results obtained through these three approaches agreed with each other, but discrepancies also became apparent. Each technique has its advantages and limitations. Analysis of promoter::*GUS* transgenic lines provided precise tissue- and cell-specificity of *AtMLO* gene expression. However, the procedure excludes a possible involvement of introns, untranslated regions and methylation of the regulatory regions of these genes in regulating expression, and does not reflect post-transcriptional regulation of mRNA levels. RT-PCR and gene expression profiling using microarray report the actual presence and accumulation of *AtMLO* transcripts, but are semi-quantitative, having low spatial resolution, and hard to avoid wounding. Since *AtMLO*s may be regulated differently by a variety of biotic and/or abiotic stimuli, different growth/experimental conditions in different labs may also cause differences in the expression of these genes.

Diversity in the expression of *AtMLO*s suggests involvement in various aspects of plant development, supporting the hypothesis that mediating disease in leaf tissues is not the primary function of AtMLO proteins. It also suggests special function(s) of each individual AtMLO, although based on the presence of common sequence motifs (e.g. the C-terminal calmodulin binding domain found in all MLOs; Kim *et al.*, 2002) a common mechanistic principle of all AtMLOs at the molecular level appears likely. The expression of several closely-related *AtMLO*

genes showed similar or overlapping tissue and developmental specificity suggesting function relatedness, i.e. (partial) functional redundancy, co-function, or antagonistic function(s), among genes within clades.

Preliminary evidence from reverse genetic studies supports both functional redundancy and co-function of AtMLO proteins. Analysis of *Atmlo5 Atmlo9* double mutant plants suggested that these two genes, both of which are expressed at high levels in pollen, may function redundantly in the process of pollen germination (Panstruga, 2005). It was also found that disruption of *AtMLO2* conferred enhanced resistance against several powdery mildew species that colonize Arabidopsis (Panstruga, 2005), whereas disruptions in *AtMLO6* and/or *AtMLO12* did not confer detectable differences (R. Panstruga, unpublished data). However, *Atmlo2 Atmlo6* or *Atmlo2 Atmlo12* double mutants exhibited higher degrees of resistance to the pathogens, and *Atmlo2 Atmlo6 Atmlo12* triple mutant plants are the most resistant (R. Panstruga, unpublished data). These results indicate that not only AtMLO2 but also AtMLO6 and AtMLO12 are involved in mediating the vulnerability of Arabidopsis plants to fungal pathogens. Recently, it was observed that *Atmlo4* and *Atmlo11* mutants exhibited similar defects in root development as did *Atmlo4 Atmlo11* double mutant plants (Z. Chen, M-J. Wu, H. A. Hartmann, P. Schulze-Lefert, R. Panstruga and A. M. Jones, unpublished data), suggesting a co-function of these two genes.

Barley MLO was shown recently to genetically and biochemically interact with the plasma membrane-localized syntaxin ROR2, Required for MLO Resistance 2 (Collins *et al*., 2003; Bhat *et al*., 2005; Panstruga, 2005). Several AtMLO proteins were also found to directly interact with the *Arabidopsis* syntaxin PEN1 (PENETRATION1) protein that resembles barley ROR2 (Schulze-Lefert, 2004). Since syntaxin belongs to the superfamily of SNARE (Soluble-N-ethylmaleimide-sensitive fusion protein Attachment protein Receptor) proteins that mediate membrane fusion of vesicles, it was proposed that MLO may modulate SNARE protein-dependent and vesicle transport-associated processes (Schulze-Lefert, 2004; Panstruga, 2005). This would indirectly affect the apoplast environment including cell wall properties. Our study examining staining patterns of *AtMLO* promoter::*GUS* lines reveals *AtMLO* expression in places where cell wall modification is likely to be occurring. These places include the valve margins of elongating fruits, the connective tissues between seed and funiculus, vascular tissues, pollen grains, the abscission zone of the floral organs and sites of excision. Therefore, results from expression analysis of *AtMLO* genes support the proposed MLO function in modulating vesicle trafficking in the context of plant development.

Acknowledgements

We thank Jing Yang, Monica Gonzalez and Tameca Sutton, all of UNC, for genotyping and processing *AtMLO* promoter::*GUS* lines and Zhi Zhang at BASF (Research Triangle Park, North Carolina) for assistance in the PLACE promoter motif analysis. This work was supported by The National Institute of General Medical Sciences (GM65989), The National Science Foundation (NSF0209711) to A.M.J., and by funds from The Max-Planck Society to H.A.H., P.S-L. and R. P.

References

The Arabidopsis Genome Initiative 2000. Analysis of the genome sequence of the flowering plant *Arabidopsis thaliana*. Nature (London) 408: 796–815.

Bechtold, N. and Pelletier, G. 1998. *In planta Agrobacterium*-mediated transformation of adult *Arabidopsis thaliana* plants by vacuum infiltration. Methods Mol. Biol. 82: 259–266.

Bhat, R.A., Miklis, M., Schmelzer, E., Schulze-Lefert, P. and Panstruga, R. 2005. Recruitment and interaction dynamics of plant penetration resistance components in a plasma membrane microdomain. Proc. Natl. Acad. Sci. USA 102: 3135–3140.

Bockaert, J. and Pin, J.P. 1999. Molecular tinkering of G protein-coupled receptors: an evolutionary success. EMBO J. 18: 1723–1729.

Breitwieser, G.E. 2004. G protein-coupled receptor oligomerization: implications for G protein activation and cell signaling. Circ. Res. 94: 17–27.

Büschges, R., Hollricher, K., Panstruga, R., Simons, G., Wolter, M., Frijters, A., van Daelen, R., van der Lee, T., Diergaarde, P., Groenendijk, J., Töpsch, S., Vos, P., Salamini, F. and Schulze-Lefert, P. 1997. The barley *Mlo* gene: a novel control element of plant pathogen resistance. Cell 88: 695–705.

Chen, J.G., Willard, F.S., Huang, J., Liang, J., Chasse, S.A., Jones, A.M. and Siderovski, D.P. 2003. A seven-transmembrane RGS protein that modulates plant cell proliferation. Science 301: 1728–1731.

Clough, S.J. and Bent, A.F. 1998. Floral dip: a simplified method for *Agrobacterium*-mediated transformation of *Arabidopsis thaliana*. Plant J. 16: 735–743.

Collins, N.C., Thordal-Christensen, H., Lipka, V., Bau, S., Kombrink, E., Qiu, J.L., Huckelhoven, R., Stein, M., Freialdenhoven, A., Somerville, S.C. and Schulze-Lefert, P. 2003. SNARE-protein-mediated disease resistance at the plant cell wall. Nature 425: 973–977.

Davuluri, R.V., Sun, H., Palaniswamy, S.K., Matthews, N., Molina, C., Kurtz, M. and Grotewold, E. 2003. AGRIS: Arabidopsis gene regulatory information server, an information resource of Arabidopsis *cis*-regulatory elements and transcription factors. BMC Bioinformatics 4: 25.

Devoto, A., Piffanelli, P., Nilsson, I., Wallin, E., Panstruga, R., von Heijne, G. and Schulze-Lefert, P. 1999. Topology, subcellular localization, and sequence diversity of the Mlo family in plants. J. Biol. Chem. 274: 34993–35004.

Devoto, A., Hartmann, H.A., Piffanelli, P., Elliott, C., Simmons, C., Taramino, G., Goh, C.S., Cohen, F.E., Emerson, B.C., Schulze-Lefert, P. and Panstruga, R. 2003. Molecular phylogeny and evolution of the plant-specific seven-transmembrane MLO family. J. Mol. Evol. 56: 77–88.

Elliott, C., Muller, J., Miklis, M., Bhat, R.A., Schulze-Lefert, P. and Panstruga, R. 2005. Conserved extracellular cysteine residues and cytoplasmic loop–loop interplay are required for functionality of the heptahelical MLO protein. Biochem. J. 385: 243–254.

Higo, K., Ugawa, Y., Iwamoto, M. and Korenaga, T. 1999. Plant *cis*-acting regulatory DNA elements (PLACE) database: 1999. Nucleic Acids Res. 27: 297–300.

Hudson, M.E. and Quail, P.H. 2003. Identification of promoter motifs involved in the network of phytochrome A-regulated gene expression by combined analysis of genomic sequence and microarray data. Plant Physiol. 133: 1605–1616.

Jones, J.D., Shlumukov, L., Carland, F., English, J., Scofield, S.R., Bishop, G.J. and Harrison, K. 1992. Effective vectors for transformation, expression of heterologous genes, and assaying transposon excision in transgenic plants. Transgenic Res. 1: 285–297.

Josefsson, L.G. and Rask, L. 1997. Cloning of a putative G-protein-coupled receptor from *Arabidopsis thaliana*. Eur. J. Biochem. 249: 415–420.

Karimi, M., Inze, D. and Depicker, A. 2002. GATEWAY vectors for Agrobacterium-mediated plant transformation. Trends Plant Sci. 7: 193–195.

Kim, M.C., Panstruga, R., Elliott, C., Muller, J., Devoto, A., Yoon, H.W., Park, H.C., Cho, M.J. and Schulze-Lefert, P. 2002. Calmodulin interacts with MLO protein to regulate defence against mildew in barley. Nature 416: 447–451.

Ma, H. 1994. GTP-binding proteins in plants: new members of an old family. Plant Mol. Biol. 26: 1611–1636.

Malamy, J.E. and Benfey, P.N. 1997. Organization and cell differentiation in lateral roots of *Arabidopsis thaliana*. Development 124: 33–44.

Mason, M.G. and Botella, J.R. 2000. Completing the heterotrimer: isolation and characterization of an *Arabidopsis thaliana* G protein gamma-subunit cDNA. Proc. Natl. Acad. Sci. USA 97: 14784–14788.

Mason, M.G. and Botella, J.R. 2001. Isolation of a novel G-protein gamma-subunit from *Arabidopsis thaliana* and its interaction with Gbeta. Biochim. Biophys. Acta 1520: 147–153.

Pandey, S. and Assmann, S.M. 2004. The Arabidopsis putative G protein-coupled receptor GCR1 interacts with the G protein alpha subunit GPA1 and regulates abscisic acid signaling. Plant Cell 16: 1616–1632.

Panstruga, R. 2005. Serpentine plant MLO proteins as entry portals for powdery mildew fungi. Biochem. Soc. Trans. 33: 389–392.

Panstruga, R. and Schulze-Lefert, P. 2003. Corruption of host seven-transmembrane proteins by pathogenic microbes: a common theme in animals and plants? Microbes Infect. 5: 429–437.

Pease, J.E. and Murphy, P.M. 1998. Microbial corruption of the chemokine system: an expanding paradigm. Semin. Immunol. 10: 169–178.

Piffanelli, P., Zhou, F., Casais, C., Orme, J., Jarosch, B., Schaffrath, U., Collins, N.C., Panstruga, R. and Schulze-Lefert, P. 2002. The barley MLO modulator of defense and cell death is responsive to biotic and abiotic stress stimuli. Plant Physiol. 129: 1076–1085.

Schulze-Lefert, P. 2004. Knocking on the heaven's wall: pathogenesis of and resistance to biotrophic fungi at the cell wall. Curr. Opin. Plant Biol. 7: 377–383.

Smith, S.M., Fulton, D.C., Chia, T., Thorneycroft, D., Chapple, A., Dunstan, H., Hylton, C., Zeeman, S.C. and Smith, A.M. 2004. Diurnal changes in the transcriptome encoding enzymes of starch metabolism provide evidence for both transcriptional and posttranscriptional regulation of starch metabolism in Arabidopsis leaves. Plant Physiol. 136: 2687–2699.

Terrillon, S. and Bouvier, M. 2004. Roles of G-protein-coupled receptor dimerization. EMBO Rep. 5: 30–34.

Turk, E.M., Fujioka, S., Seto, H., Shimada, Y., Takatsuto, S., Yoshida, S., Denzel, M.A., Torres, Q.I. and Neff, M.M. 2003. CYP72B1 inactivates brassinosteroid hormones: an intersection between photomorphogenesis and plant steroid signal transduction. Plant Physiol. 133: 1643–1653.

Weiss, C.A., Huang, H. and Ma, H. 1993. Immunolocalization of the G protein alpha subunit encoded by the *GPA1* gene in Arabidopsis. Plant Cell 5: 1513–1528.

Zimmermann, P., Hirsch-Hoffmann, M., Hennig, L. and Gruissem, W. 2004. GENEVESTIGATOR. Arabidopsis microarray database and analysis toolbox. Plant Physiol. 136: 2621–2632.